Summer Student Program
Joint Institute for Nuclear Research

Dzhelepov Laboratory of Nuclear Problems

Ring artifact reduction on cone beam MARS CT Scanner

Arnold Weiszenbacher
Babes-Bolyai University of Cluj-Napoca, Romania

Supervisor: Alexey ZHEMCHUGOV

Dubna, 2015

Contents

Introduction

The purpose of this practice was to reduce ring artifact contribution to the reconstruction of 2D images obtained from the MARS CT Scanner through means of the Medipix3 detector.

The MARS scanner is designed for the x-ray spectroscopic study of samples with the aid of computer tomography methods. Computer tomography allows the reconstruction of slices of an investigated sample using a set of shadow projections obtained for different angles. Projections in the MARS scanner are produced using a cone x-ray beam geometry. The MARS (Medipix All Resolution System) scanner obtained by the Laboratory of Nuclear Problems of the Joint Institute for Nuclear Research, has a camera with two detectors based on gallium arsenide (compensated with chromium) and equipped with the Medipix3.1 electronics. The Medipix3.1 electronics can simultaneously count the number of photons with energies above the threshold at each pixel for two different thresholds.[1] Each detector has effective dimensions of 14 mm x 14 mm, it is designed using a commercial 0.13 micrometers CMOS technology with eight metal layers and each sensitive area contains a matrix of 256 x 256 pixels of 55 microns.[2]

Ring artifacts are the concentric rings superimposed on the tomographic images often caused by the defective and insufficient calibrated detector elements.[3] Other factors which may contribute include dark image, gain non-uniformity due to submodules or changes in temperature and beam strength.[4] Ring artifacts are evident in the reconstructed image as narrow rings or wide bands. If 360 degree data acquisition is used, they appear as arcs of different lenth.[5] Most corrections in literature are split into main categories, one based on sinogram processing and the other based on the reconstructed 2-D images.[6] A sinogram is obtained by taking all different views of the projection data and staking them one upon the other. Each column thus represents a single pixel, observed in different time positions.[7] Both defective and malfunctioning pixels on the sinograms as well as the reduction of rings on the reconstructed images were quantified perceptually.

Method

Different algorithms were applied on the sinograms in order to correct defective and malfunctioning pixels while raw images were used in order to identify the defective chip areas, with further processing being able to diminish the latter's influence on ring artifact generation. Programming was done in C++ language and FreeImage library was used in order to load the images, while Minuit library was used for optimization purposes. Moreover, all images were processed with ImageJ software.

All corrections were made on images obtained with the MARS CT Scanner, from the Department of Colliding Beam Physics of Dzhelepov Laboratory of Nuclear Problems, Joint Institute of Nuclear Research. The project involved two different stages. For the first stage of the project, corrections were done on the sinograms obtained through MPPC Software. The sinograms were previously corrected for darkfield and flatfield. For the second stage, raw projections were first used in order to identify the boundaries of the malfunctiong chips and then these were later identified on the sinograms and corrections were applied.

In the first stage defective and malfunctioning pixels were identified on the sinograms and 4 different filters were tested for correction. A mean filter, median filter, a column filter and a pixel filter were applied. A bilinear interpolation algorithm provided the same results as the mean filter.

For the median filter, the whole image is scanned pixel by pixel, replacing each pixel value with the median of the neighboring pixel values. This is achieved through a window of custom size which slides along the entire image. Median filtering is especially effective in removing salt and pepper noise.[8]

Mean filtering works in a similar manner, with the exception being that each pixel value in the image is replaced with the average of its neighbors. This usually happens in a kernel which gives the shape and size of the neighboring sample.[9]

For the column filter, another sliding window with custom geometry was chosen and the whole image was scanned with it. Means for the whole columns in the window were computed and the difference between the mean of the central column and the median of the column means was compared against the square root of the sum of errors in order to find an appropriate threshold for identification of defective pixels. Those thus identified were then normalized with respect to the median value. The median was chosen as a reference instead of the mean because it provides a better indicator of the magnitude of the jumps in intensity.

The pixel algorithm is based on the same process with the sole exception consisting in comparing the central value of the central column against the median of the column means in the same designated window.

In the second stage, the boundaries of the malfunctioning chip are detected from the raw images, their position is then determined on the filtered sinograms and the defective lines from the bad area of the chip are corrected before reconstruction. A five degree polynomial was used for optimization in order to correct the defective columns from the damaged chip area. Line fitting was done in a 30 pixel column and Minuit library [10] was used for function minimization, with subsequent normalization for the defective pixels. This technique is useful for discriminating between bad columns from the damaged chip and the contribution of the overlapping object that is being scanned. Thus only those portion of the chip area that are malfunctioning are corrected and no loss of information occurs.

In order to further enhance the image, a 21 column sliding windows was then used in which the central column was normalized with respect to the mean of the other columns with the help of a user-defined threshold. Moreover, a 3D correction was then applied in which a sliding window of 3 columns was used for 3 consecutive sinograms. The central column in the window from the central sinogram was normalized with respect to the mean of the other 8 columns from the corresponding sinograms.

Reconstructions were generated from the processed sinograms using Octopus Software and the extent of ring reduction was quantified.

Results and Discussion

For the first stage we conclude the column filter to be the most appropriate in correcting the defective columns on the sinogram. The correction was successful without further deleterious effects on the overall image quality. Conventional methods such as the mean and median filters perform poorly with significant information lost either by smoothing detailed features or by introducing more artifacts in the reconstructions. However, these algorithms can be used for removing salt and pepper noise at the end of processing, thus adding further quality to the image, even though they do not contribute to overall ring artifact reduction.

Figure 1.1 Sinogram no.21 before column filter

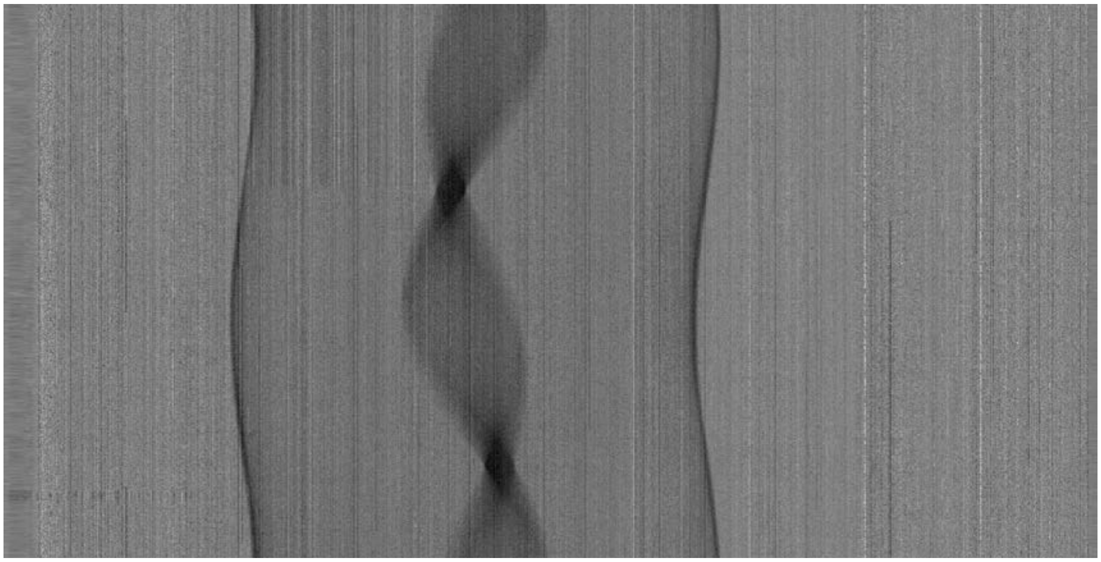

Figure 1.2 Sinogram no.21 after column filter

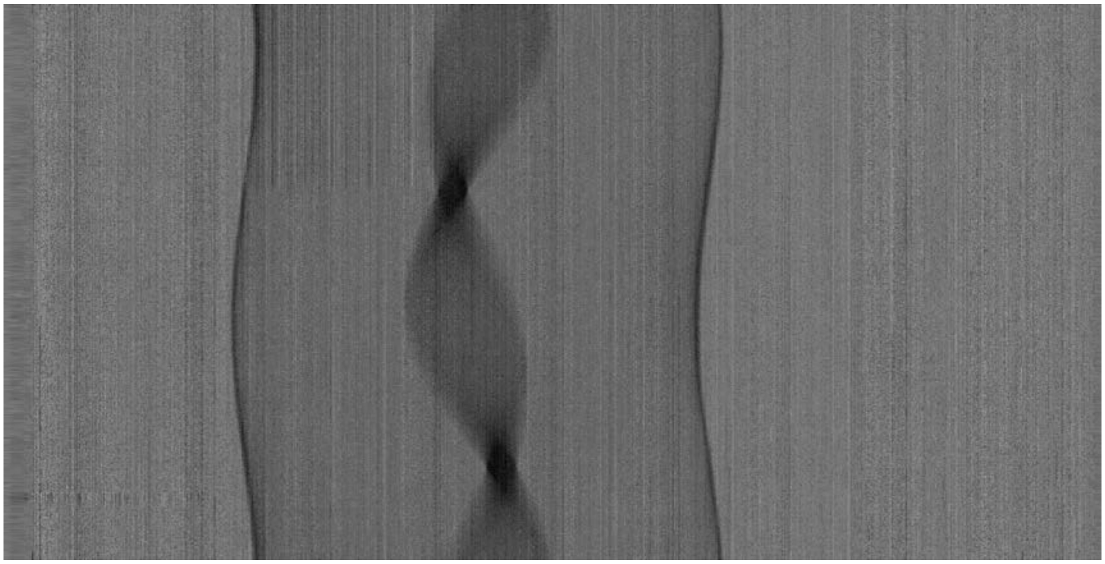

Figure 1.3 Intensity profiles for the two sinograms

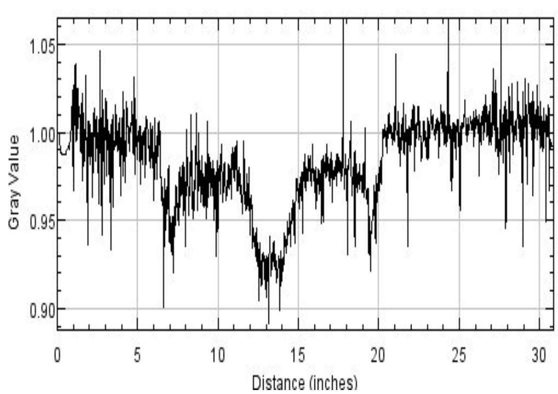

Fig.1.3.1 Intensity profile before correction

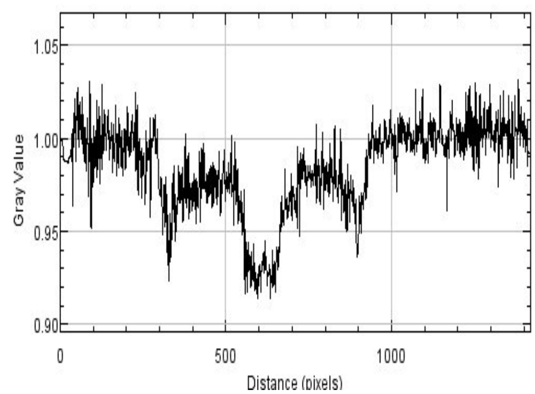

Fig.1.3.2 Intensity profile after correction

In the second stage, in order to distinguish the jumps in intensity due to malfunctioning pixels at different positions from those due to absorption by the object, a 5 degree polynomial was used for nonlinear approximation in a column of 30 pixels, with its center at the horizontal border between the defective chip and the functioning one. Function minimization was achieved with the help of the Minuit library and each pixel value from the malfunctioning columns of the chip was normalized with respect to the jump coefficient. The processing time for the optimization of all 257 sinograms was 42 seconds with an average of 0.163 seconds per image, thus making it feasible for practical applications.

Figure 2.0 Processing time for optimization

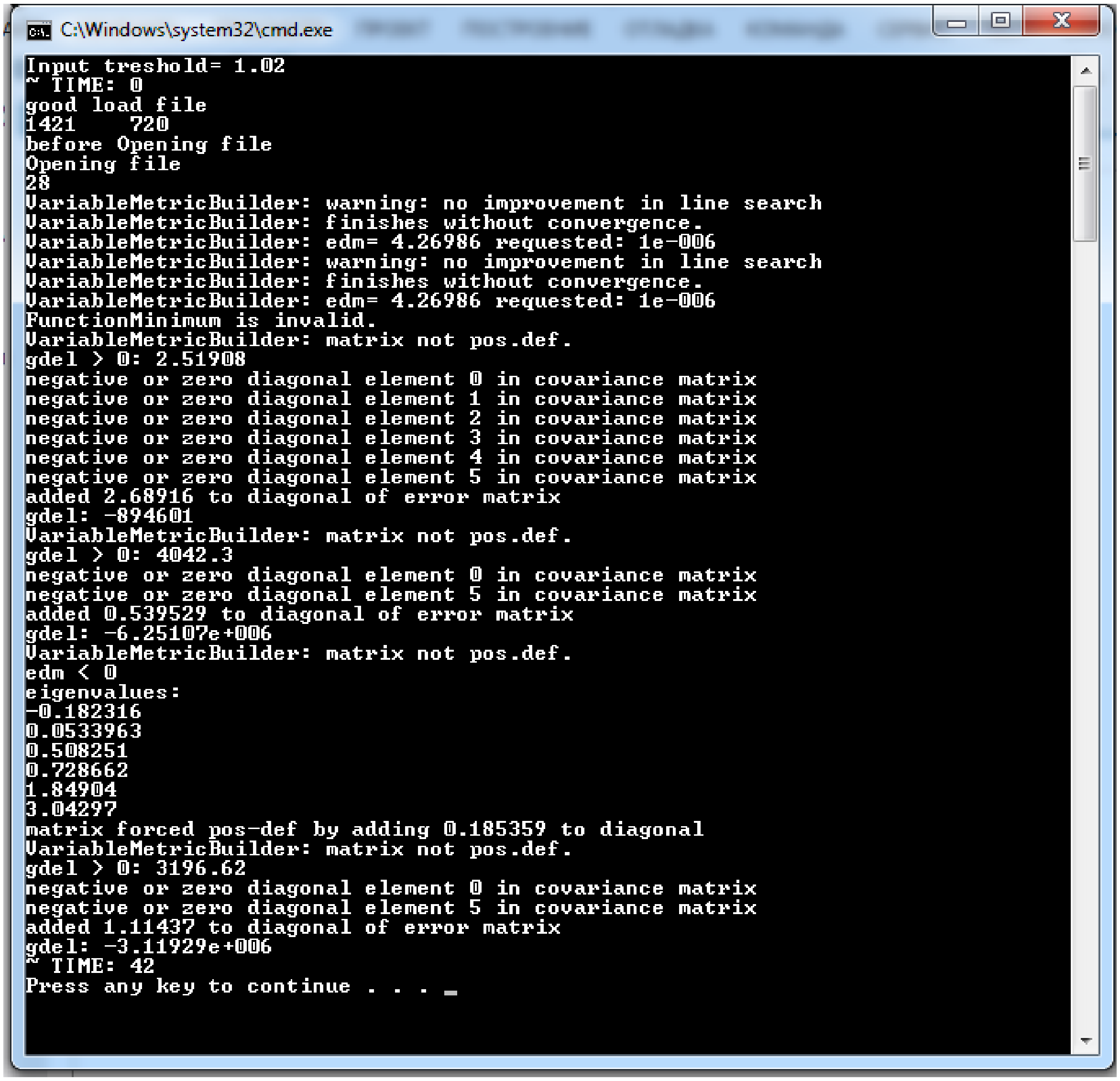

Figure 2.1.1 Sinogram no.21 before optimization

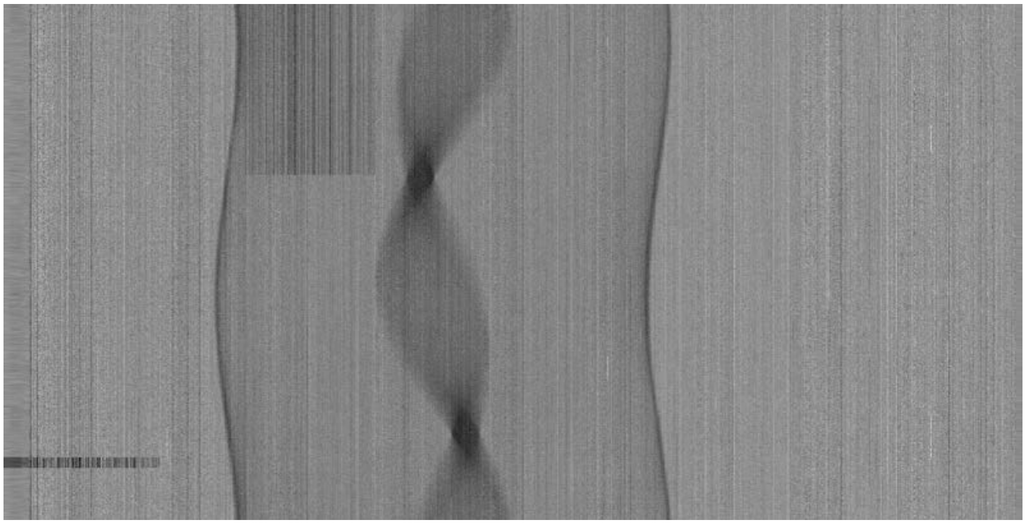

Figure 2.1.2 Sinogram no.21 after optimization

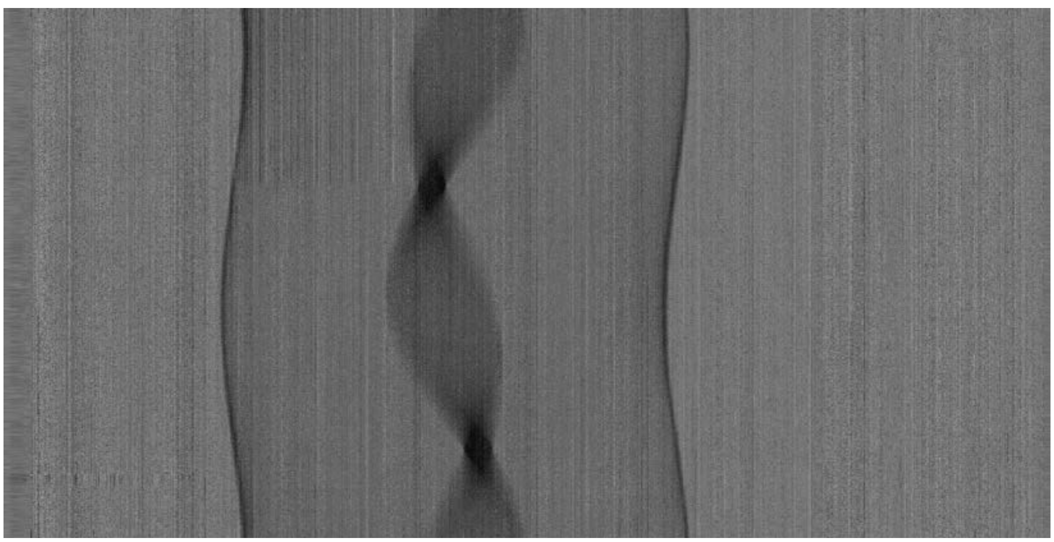

After optimization, the overall effect of the next 2 algorithms was to dampen the peaks in the intensity profile and to provide a more smoothed image for the next stage of processing.

Figure 2.2.1 Intensity profile before dampening

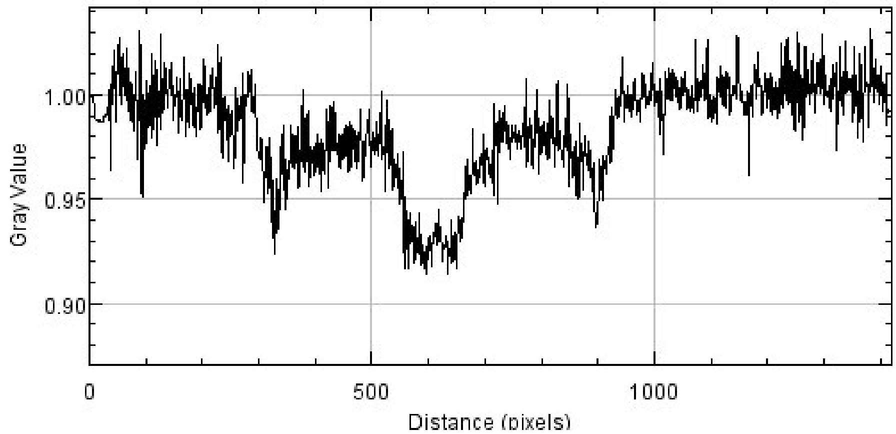

Figure 2.2.2 Intensity profile after dampening

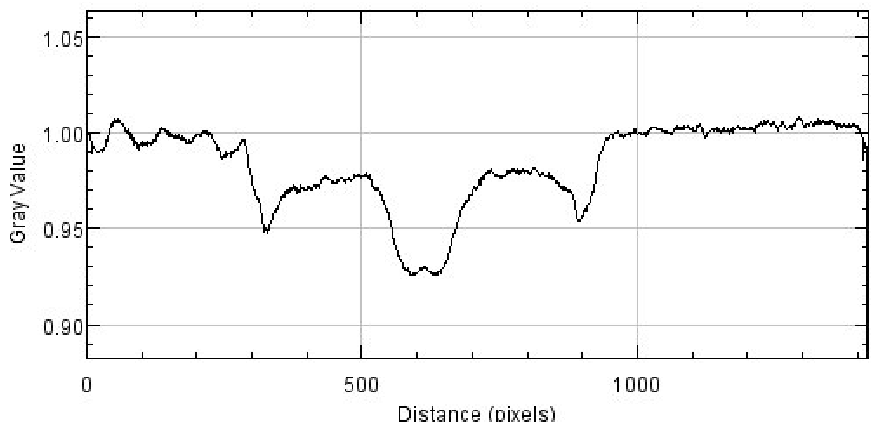

Figure 2.2.3 Final version of sinogram no.21 after all corrections

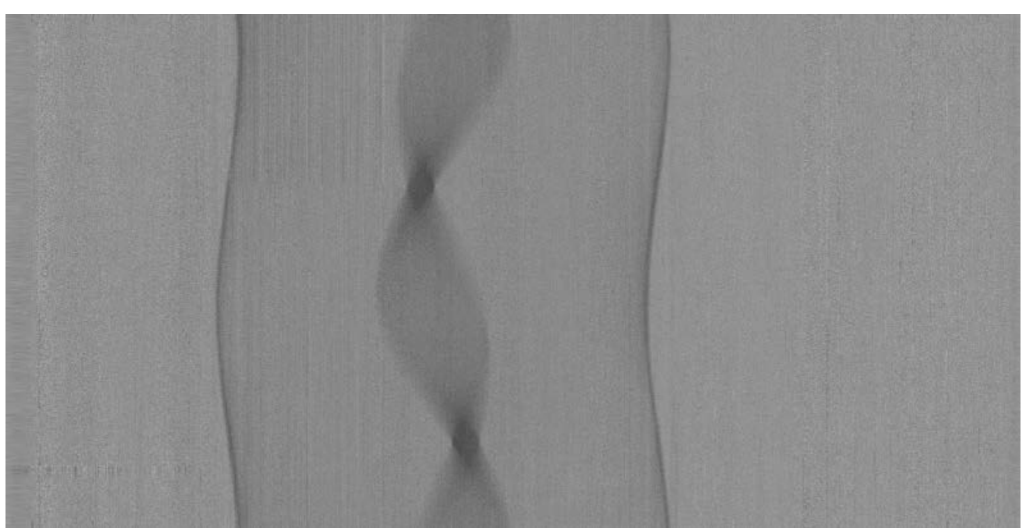

After first applying the column filter and then using the optimization process described in the second stage, as well as the algorithms for dampening the intensity profile, the processed sinograms were then used for 2D reconstructions. Significant reduction of concentric rings in the processed image was observed. A plugin for polar coordinates was used in ImageJ in order to better visualize the extent of ring generation in the reconstructions. [11]

Figure 3.1.1.1 Reconstruction before correction no.54

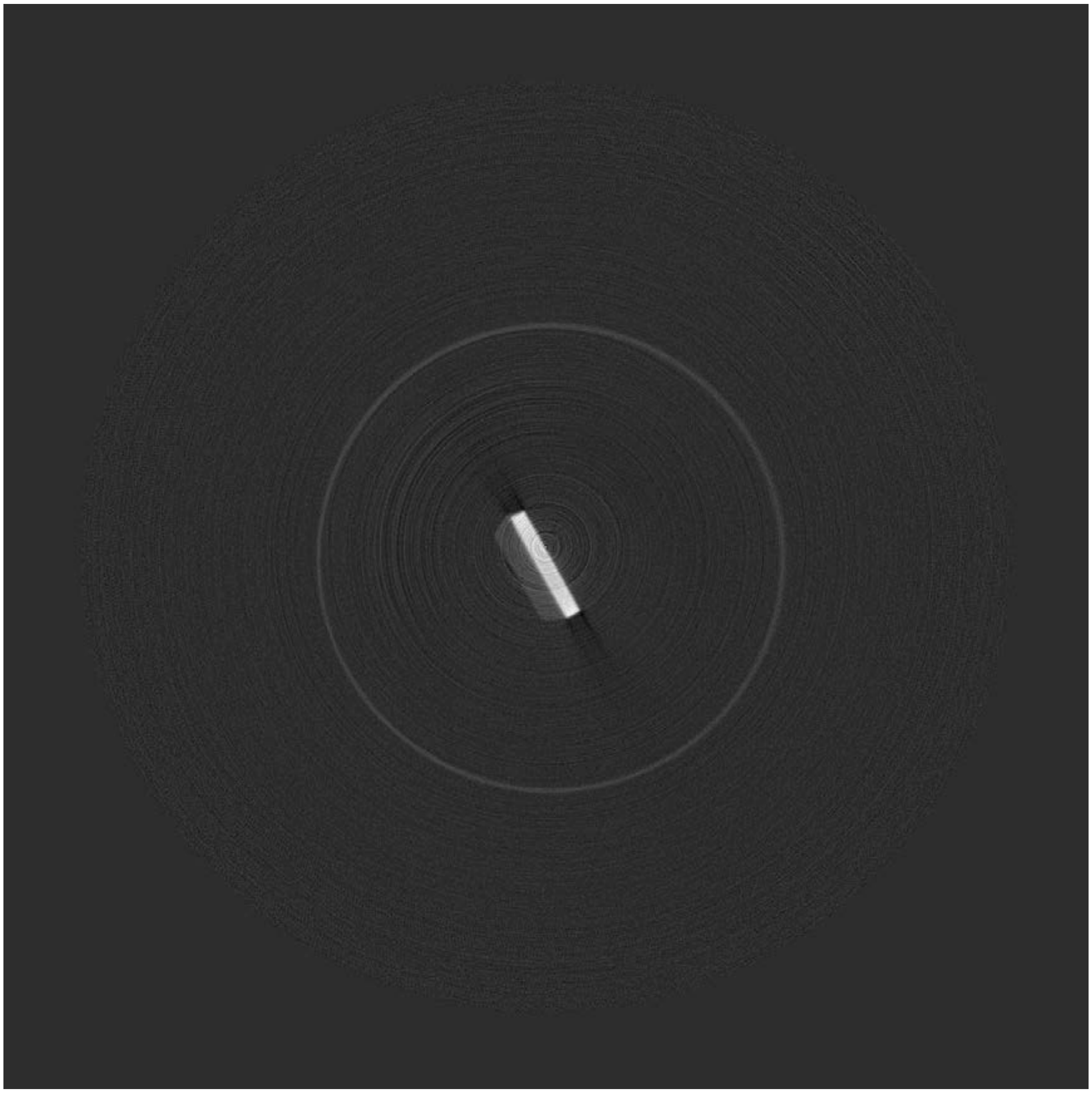

Figure 3.1.1.2 Reconstruction after correction no.54

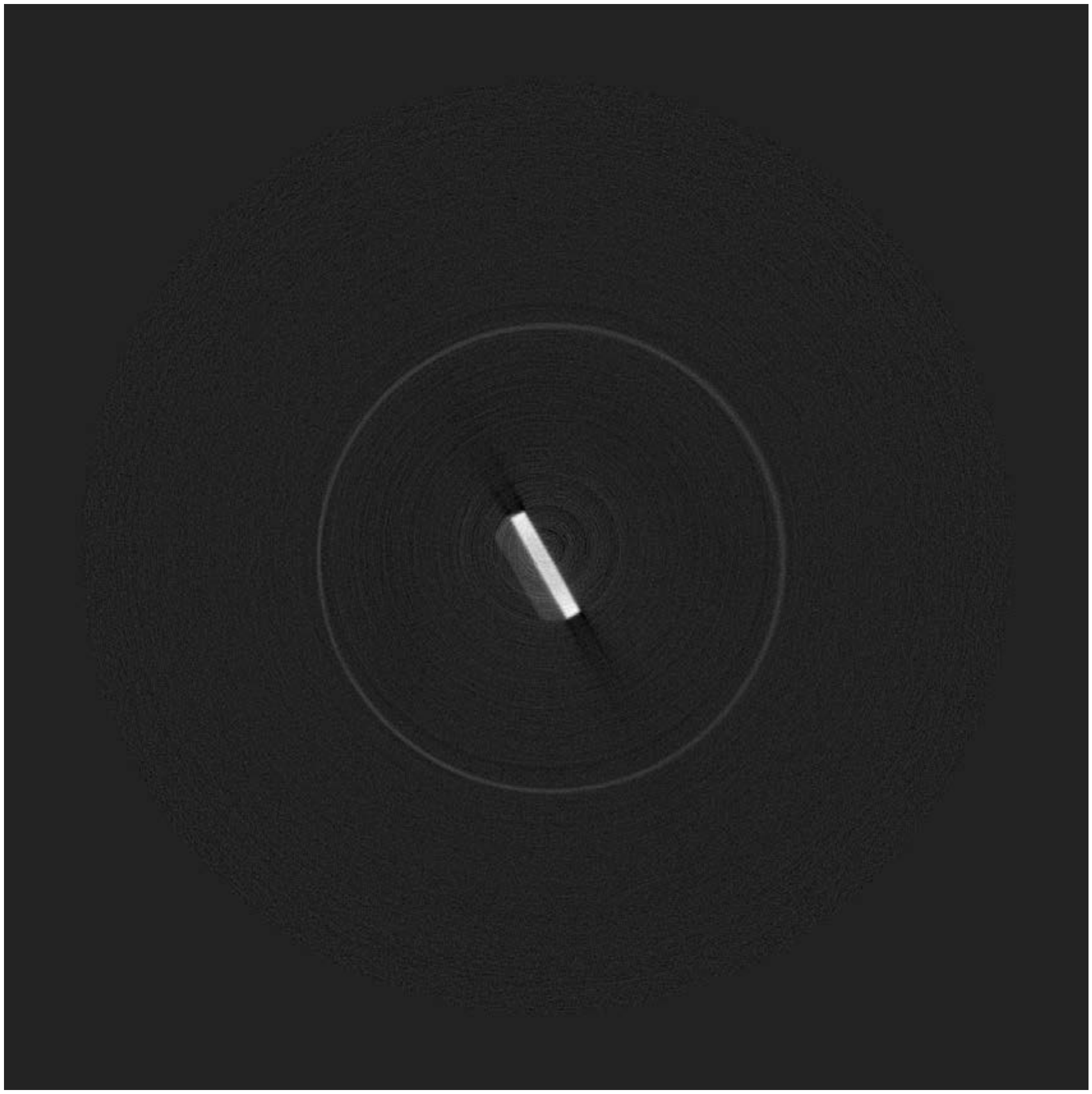

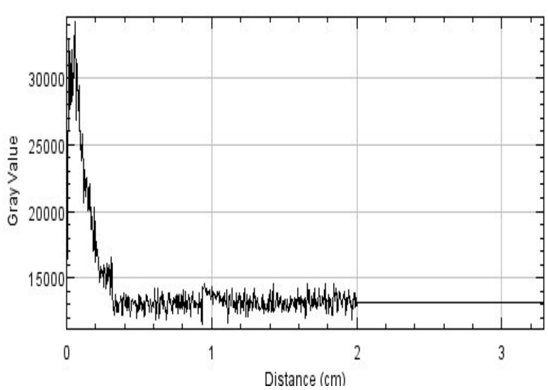

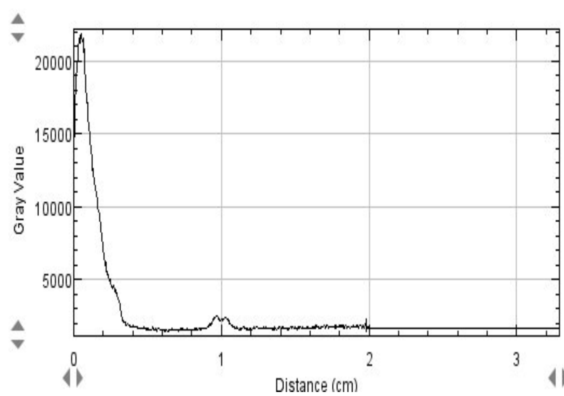

Figure 3.1.2.1 Profile before correction no.54 Figure 3.1.2.2 Profile after correction no.54

Figure 3.2.1.1 Reconstruction before correction no.72

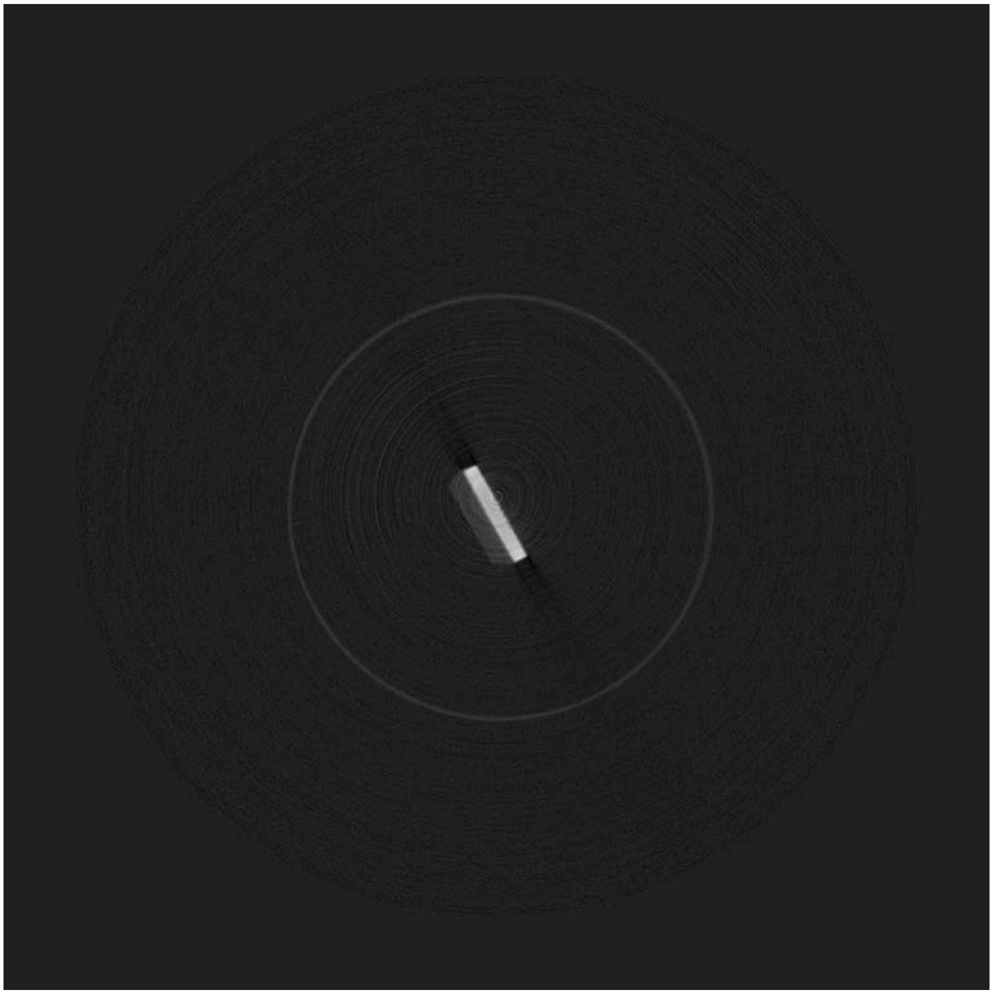

Figure 3.2.1.2 Reconstruction after correction no.72

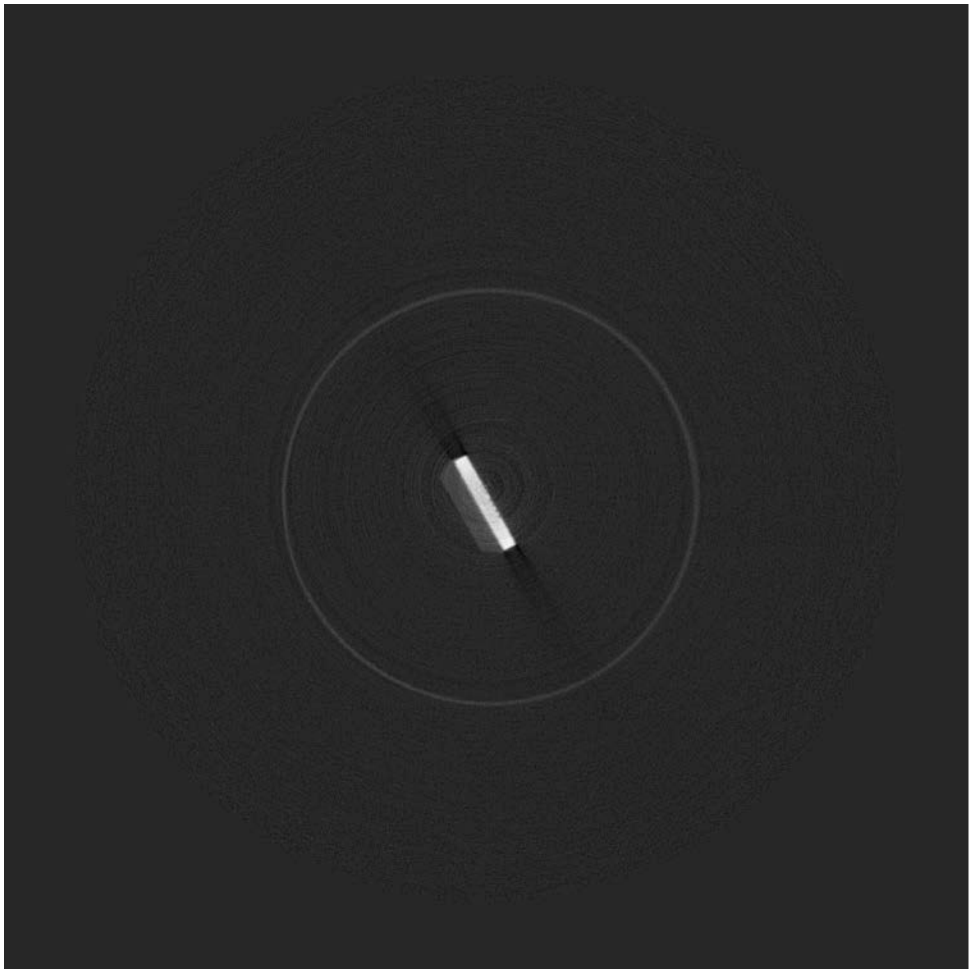

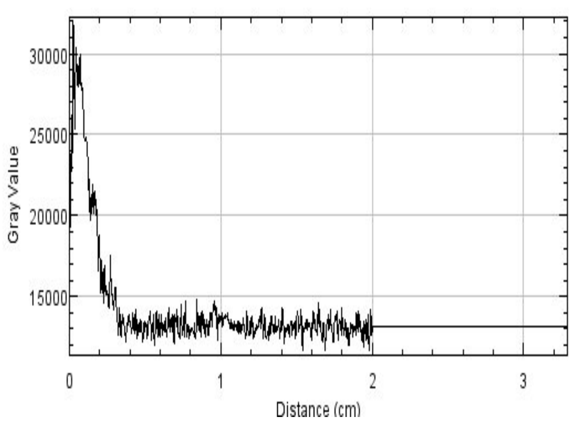

Figure 3.2.2.1 Profile before correction no.72

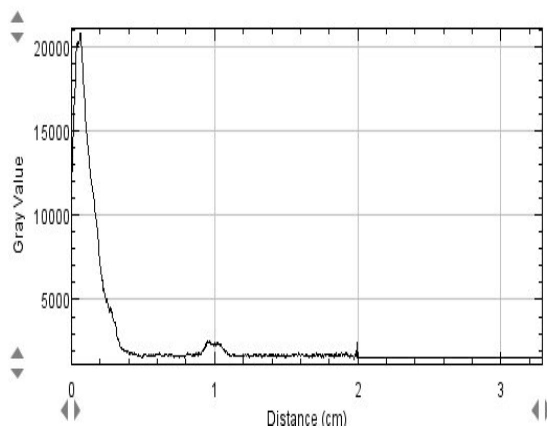

Figure 3.2.2.2 Profile after correction no.72

Conclusions

We have found the chip to malfunction in certain positions. Since not all pixels malfunction in the defective chip area we can safely dismiss the hypothesis of problems regarding voltage supply. However, the nature of these disturbance is left to debate.

Sinogram-domain-based ring artifact correction, coupled with identification of the position of the malfunctioning chips from the raw images and subsequent correction in the sinogram domain seems to provide an efficient method for diminishing ring artifact contribution on the reconstructed images. A column filter offers the best results for removal of defective pixels from the original sinograms while optimization provides the most satisfactory results for identification and subsequent correction of the malfunctioning pixels in the defective area of the chip.

Malfunctioning chip boundaries can be determined from the raw images and later identified on the sinograms, thus providing the necessary encroachment of the bad regions in the sinogram.

Acknowledgements

I would like to express my appreciation to Prof. Alexey Zhemchugov, my practice supervisor as well as to Prof. Georgy Shelkov, for giving me an opportunity to participate in the 2015 Student Summer Program at JINR.

I would also like to thank Danila Kozhevnikov, Igor Denisenko and Andrei Gridin, my colleagues, for their support and knowledge sharing. On top of all this, I would like to thank Elena Karpova for providing me with useful information and helping me with all the papers.

References

[1] A. Gongadze, A. Zhemchugov, G. Chelkov, et. al, (**2015**).*Alignment and resolution studies of a MARS scanner*
[2] R. Ballabriga et al., *Nuclear Instruments and Methods in Physics Research A*, (**2011**), 633:S15–S18
[3] F. Boas, D. Fleischmann, *Imaging Med.* (**2012**), 4(2):229-240
[4] J.H. Siewerdsen and D.A. Jaffray, (**1999**), *Med. Phys.*, 26:2635–47
[5] R. A. Ketcham, *SPIE*, (**2006**), 6318: 63180O1
[6] A. Anas et al., *BioMedical Engineering OnLine*, (**2011**), 10:72
[7] J. Hsieh, SPIE Press, (**2003**) 167.
[8] F. Sadi, S. Y. Lee, and M. K. Hasan, *Comput. Biol. Med*. (**2010**). 40(1):109–118.
[9] A. Buades, B. Coll, J.M. Morel, *Multiscale Modeling and Simulation*, (**2005**), 4(2):490-530
[10] http://seal.web.cern.ch/seal/snapshot/work-packages/mathlibs/minuit/ (Accesed on **19.08.2015**)
[11] http://rsb.info.nih.gov/ij/plugins/polar-transformer.html (Accesed on **20.08.2015**)